A comment on "Orogen-parallel, active left-slip faults in the Eastern Himalaya: Implications for the growth mechanism of the Himalayan Arc" by Li and Yin (Earth Planet Sci. Lett. 274 (2008) 258-267).

J. Van der Woerd[a], Ph.-H. Leloup[b], Liu-Zeng J.[c], R. Lacassin[d], P. Tapponnier[d]

[a] Institut de physique du Globe de Strasbourg, UMR CNRS/UdS 7516, 5, rue Descartes 67084 Strasbourg, France.

[b] Laboratoire des Sciences de la Terre, CNRS UMR 5570, UCB Lyon1-ENS Lyon, Lyon, France.

[c] Institute of Tibetan Plateau Research, Chinese Academy of Sciences, Beijing, China

[d] Institut de Physique du Globe de Paris, CNRS UMR 7154, Paris, France.

23 Feb 2009

1. Introduction

Understanding how convergence is partitioned in the Himalayan arc and across the entire Tibetan plateau provides critical kinematic constraints on mechanical models of continental lithospheric deformation. Based on geomorphic evidence, Li and Yin (2008) recently claimed to have discovered several active E-W trending left-lateral faults in South Tibet. These faults, interpreted to be part of a ~100 km-wide and >500 km-long Dinggye–Chigu fault zone (DCFZ), would follow the Himalayan arc from ~88°E to the eastern syntaxis (95°E). The total slip-rate across this zone would be at least 4 to 8 mm/yr, and possibly up to 25 to 70 mm/yr (when summing given slip-rate on each fault). The rates are then compared with the right-lateral slip-rate along the Karakorum fault in western Tibet, inferred to be between 1 and 10 mm/yr from the literature. It is concluded that, since 4 Ma,

oroclinal bending is the dominant process in Himalayan tectonics (Klootwijk et al., 1985).

This article has major implications on the mechanics of the Himalayas and of the collision belts in general. **Our fieldwork, geomorphic and geodetic analysis of the region studied by Li and Yin (2008) suggest: 1) the geomorphic features presented by these authors are better explained by the alignment of landforms that have no tectonic origin,** 2) GPS and earthquake data do not support E-W left-lateral shear in South Tibet and 3) there is no evidence for active left-lateral shearing so far in the region west of the eastern Himalayan syntaxis.

2. Active fault mapping, and geomorphic offsets.

A first and fundamental step in the study of Li and Yin (2008) is to map five previously unrecognized active faults. **We suggest many of the faults mapped by Li and Yin (2008) are paleo shorelines or other geomorphic features with no tectonic origin.** Several faults said to be active have no distinguishable trace on high-resolution images and do not show typical features of active strike-slip fault such as mole tracks or pull-apart depressions. The authors do not provide evidence other than supposed deflected streams, deflected smooth terrace risers, or offset shorelines, but these deflections are not systematic and sometimes indicate opposite senses along a given fault. We will show that all geomorphic elements presented by the authors as evidence for active faulting are ambiguous and may be interpreted in a completely different way. Such demonstration can easily be performed using the Google Earth™ imagery and we briefly show some examples below.

The South Gongzuo fault (CGF) is mapped as a range bounding structure, between the Gongzuo basin (~4500 m *asl*) and the high range of the Kangchengjunga foothills (~5100 m *asl;* Fig. 1). The fault is interpreted as left-lateral, offsetting streams by 500 to 3500 m

50 (Fig. 4 in Li & Yin, 2008). In fact, the mapped fault exhibits a left-stepping geometry
51 untypical of strike-slip faults and the range front is rather smooth and in the absence of slope
52 break. Only 3 of the 11 stream channels crossing the fault are mapped as deflected by the
53 fault and none of these offsets is clear (see for instance Li & Yin westernmost site where their
54 Figure 4B of Li and Yin (2008) shows a marker – the valley edge – approximately aligned on
55 either side of the supposed fault trace while they claim it is offset by 2.7 km). Furthermore,
56 the fault is described as buried below the T2 fluvio-glacial deposits in which the deflected
57 channels are incised. This leads to an impossible relative timing with the fault at the same
58 time older (because buried below the deposits) and younger (because offsetting the channels
59 incised within the deposits) than the T2 deposits. We conclude that the southern boundary of
60 the Gongzuo basin is better interpreted as a passive piedmont (bajada) with no evidence of
61 active tectonics.

62 The Central Gongzuo fault (CGF) is interpreted to truncate several alluvial fans and to
63 offset left-laterally one stream channel by ~1100 m (Fig. 4 in Li & Yin, 2008). This
64 deflection, ranging from 0 m to 5.7 km when considering the whole width of the upstream
65 channel, is most likely imposed by a large bedrock outcrop lying in front of the river course
66 (Fig. 2). It cannot be used as a reliable geomorphic marker of tectonic offset. The western
67 stretch of the CGF corresponds in the field to a scarp in colluvium indurated by a calcium
68 carbonate matrix overlain by a thin sandstone level located at an elevation of 4400 m a.s.l.
69 (Figs 1 and 3). We rather interpret this deposit and the associated scarp as a paleo-shoreline
70 of a large paleo-lake that occupied a wide area of the upper Arun (or Pumqu) catchment (e.g.,
71 Wager, 1937; Armijo et al., 1986; see paleo-lake contour in Fig. 1).

72 The North Gongzuo fault (NGF) is interpreted to have offset left-laterally three
73 terraces levels by 85 to 380 m (Fig. 6 of Li and Yin, 2008). A closer examination of this area

74 (Fig. 4) reveals that a large sand ridge was mistakenly interpreted as an active river channel,
75 that mapped T1 terrace is in fact the slope of the sand ridge, that mapped T2 is the present-
76 day stream bed, and that mapped T3 is a bedrock slope. No fault scarp (mixed up with little
77 incisions) is visible, and no offset can be measured (Fig. 4).

78 The North Comuzhelin fault (NCF) is interpreted to lie on the southern flank of an E-
79 W ridge extending into the Comuzhelin lake (Fig. 5) and to offset left-laterally paleo-
80 shorelines by ~50 m (Fig. 5 of Li and Yin, 2008). A closer look to this area reveals that the
81 shorelines have been improperly mapped and exhibit an apparent right-lateral rather than left-
82 lateral offset (Fig. 5C). **In fact there is no clear evidence of any active fault in this area**
83 **and the 15° east-dipping striations shown in Figure 7A of Li and Yin (2008) do not**
84 **indicate it is an active strike-slip fault.**

85 We conclude that Li and Yin (2008) do not provide any convincing morphological
86 arguments to constrain the rate of active left-lateral faults, neither the existence of such faults.
87 The obtained Plio-Quaternary ages are thus useless to this respect.

88

89 **3. Geophysical evidence.**

90 Using GPS data from two stations published by Paul et al. (2001), Li and Yin (2008)
91 calculate a N-S shortening rate of 12 ± 3 mm/yr and an E-W left-slip rate of 2.5 ± 1.5 mm/yr
92 between a station in South Tibet (#1) and a station on stable India (#2) (Fig. 6). This appears
93 compatible with their lowest estimated slip rates. However, the authors recognize themselves
94 that the two stations are not separated by the alleged DCFZ but by the Dinggye N-S normal
95 fault and the Main Boundary Thrust (Fig. 6). Indeed, it would have been wiser to consider the
96 Lhasa (LHAS) GPS station which is separated from station #2 by the DCFZ and the Main
97 Boundary Thrust (see Fig. 2 of Li & Yin, 2008; Fig. 6). In that case the relative motion

between the two stations would combine N-S shortening and E-W right-lateral shearing or E-W extension, which is incompatible with the proposed left-lateral faults. We show more GPS sites and velocities (Zhang et al., 2004) on Figure 6, that show no evidence for left-lateral shear, and, which are more compatible with right-lateral shear, if any movement occurs across the DCFZ.

Focal mechanisms of two small earthquakes (M ~5) (Priestly et al., 2007) indicate, respectively, no shear stress and right-lateral shear on E-W vertical planes. Li and Yin (2008) try to discuss how this could be compatible with E-W left-lateral shear. This exercise is useless as the ~70 km depth of the two events locate them in the Indian subducting slab (Priestley et al., 2007; De La Torre et al., 2007; Liang et al., 2008). They have thus little to do with the state of stress in the south Tibetan crust. The upper crustal seismicity in south Tibet rather indicates almost pure N-S normal faulting with no sign of E-W left-lateral shear (e.g., Harvard GCMT; Liang et al., 2008).

4. Other evidence for left-lateral faulting in southeastern Tibet ?

Citing Ratschbacher et al. (1992, 1994), Yin (1994) and Li (1992), Li and Yin (2008) claim that evidence for E-W left-lateral faults extend to at least 92°E, defining the >500 km long DCFZ. It is also suggested that the fault zone could extend up to the eastern syntaxis where left-lateral faults were observed by Burg et al. (1998) and Ding et al. (2001) (Fig. 2 of Li and Yin, 2008). These assertions are rather surprising as most of these references are misquoted. Ratschbacher et al. (1992) contains absolutely no data about evidence for left-lateral faulting. Ratschbacher et al. (1994) describe few left-lateral brittle faults near Xigaze, close to the Yarlung-Tsangpo suture zone, but these faults occur together with conjugate right-lateral ones and indicate a N8°E compression not E-W left-lateral strike-slip faulting.

From the right-stepping geometry of the N-S normal faults in the main rift systems (i.e. Yadong-Gulu) Ratschbacher et al. (1994) and Li (1992) proposed limited component of left-lateral shear in a ~N60° direction. This direction is oblique to that proposed for the DCFZ. Burg et al. (1998) and Ding et al. (2001) describe left-lateral faults (Yiema-La and Pai) bounding to the west the eastern Himalayan syntaxis (Namche-Barwa). However, these faults extend for ~150 km at most and strike almost N-S on the western side of the syntaxis, and bend to N50°E at their southern extremity. These faults certainly do not strike N70°E for ~225 km as dumped in Fig. 2 of Li and Yin (2008).

4. Conclusion

Geomorphology is a powerful tool to evidence and characterize active deformations (e.g., Tapponnier et al., 1977; Armijo et al., 1986; Peltzer et al., 1988; Avouac et al., 1993; Gaudemer et al., 1995; Meyer et al., 1998; Van der Woerd et al., 2002). However, such analysis has to rest on careful observation of the landforms and not lead to the invention of active faults. Contrarily to what is stated by Li and Yin (2008) there is no evidence for E-W left-lateral faulting in south Tibet east of Dinggye (88°E). The present day stress field in that area corresponds to an E-W minor stress axis ($\sigma 3$) with ~N-S normal faults (e.g., Armijo et al., 1986). We conclude that there is no left-lateral DCFZ connecting south Tibet with the eastern syntaxis, which, symmetrically with the Karakorum fault, would play a major role in Himalayan arc oroclinal bending.

References

145 Armijo, R., P. Tapponnier, J.L. Mercier and Han Tong Lin, 1986. Quaternary extension in
146 southern Tibet : Field observations and tectonics implications. J. Geophys. Res. 91,
147 n°B14, 13803-13872.
148 Avouac, J.P., P. Tapponnier, M. Bai, H. You and G. Wang, 1993. Active thrusting and folding
149 along the northern Tien Shan and late Cenozoic rotation of the Tarim relative to Dzungaria
150 and Kazakhstan. J. Geophys. Res. 98B4, 6655-6804.
151 Burg, J.P., M. Brunel, D. Gapais, G.M. Chen, G.H. Liu, 1984. Deformation of leucogranites of the
152 crystalline Main Central Sheet in southern Tibet (China). J. Struct. Geol 6, 535-542.
153 Burg, J.P., P. Nievergelt, F. Oberli, D. Seward, P. Davy, J.-C. Maurin, Z. Diao, M. Meier,
154 1998. The Namche Barwa syntaxis: evidence for exhumation related to compressionnal
155 crustal folding. J. Asian Earth Sci 16, 2-3, 239-252.
156 De la Torre, T.L., G. Monsalve, A.F. Sheehan, S. Sapkota, F. Wu, 2007. Earthquake
157 processes of the Himalayan collision zone in eastern Nepal and the southern Tibetan
158 plateau. Geophys. J. Int. 171, 718-738.
159 Ding, L., D.L. Zhong, A. Yin, P. Kapp, T.M. Harrison, 2001. Cenozoic structural and
160 metamorphic evolution of the eastern Himalayan syntaxis (Namche Barwa). Earth
161 Planet Sci. Lett. 192, 423-438.
162 Gaudemer, Y., P. Tapponnier, B. Meyer, G. Peltzer, Guo S., Chen Z., Dai H., I. Cifuentes,
163 1995. Partitioning of crustal slip between linked active faults in the eastern Qilian Shan,
164 and evidence for a major seismic gap, the “Tianzhu gap”, on the western Haiyuan fault,
165 Gansu (China). Geophys. J. Int. 120, 599-645.
166 Klootwijk, C.T., P.J. Conaghan, C.M. Powell, 1985. The Himalayan arc: large-scale
167 continental subduction, oroclinal bending, and back-arc spreading. Earth Planet. Sci.
168 Lett. 75, 316-319.

169 Li, D., 1992. On tectonic asymmetrical evolution of the Himalayan orogenic belt. Earth Sci.
170 17 (5), 539-545 (in Chinese with English abstract).
171 Li, D., A. Yin, 2008. Orogen-parallel, active left-slip faults in the Eastern Himalaya:
172 Implications for the growth of the Himalayan Arc. Earth Planet. Sci. Lett. 274, 258-
173 267.
174 Liang, X., Zhou S., Y.C. Chen, G. Jin, L. Xiao, P. Liu, Y. Fu, Y. Tang, X. Lou, J. Ning,
175 2008. Earthquake distribution in southern Tibet and its tectonic implications. J.
176 Geophys. Res. 113, B12409, doi:10.1029/2007JB005001.
177 Meyer, B., P. Tapponnier, L. Bourjot, F. Métivier, Y. Gaudemer, G. Peltzer, Guo S. and Chen
178 Z., 1998. Mechanisms of active crustal thickening in Gansu-Qinghai, and oblique,
179 strike-slip controlled, northeastward growth of the Tibet plateau. Geophys. J. Int. 135,
180 1-47.
181 Peltzer, G., P. Tapponnier, Y. Gaudemer, B. Meyer, Guo S., Yin K., Chen Z., Dai H., 1988.
182 Offsets of late quaternary morphology, rate of slip, and recurrence of large earthquakes
183 on the Chang Ma fault (Gansu, China). J. Geophys. Res. 93, n°B7, 7793-7812.
184 Priestley, K., J. Jackson, D. McKenzie, 2007. Lithospheric structure and deep earthquakes
185 beneath India, the Himalaya and southern Tibet. Geophys. J. Int. 172, 345-362.
186 Ratschbacher, L., W. Frisch, C. Chen, G. Pan, 1992. Deformation and motion along the
187 southern margin of the Lhasa block (Tibet) prior to and during the India-Asia collision.
188 J. Geodyn. 16, 21-54.
189 Ratschbacher, L., W. Frisch, G. Liu, C. Chen, 1994. Distributed deformation in southern and
190 western Tibet during and after the India-Asia collision. J. Geophys. Res. 99, 19917-
191 19945.

192 Tapponnier, P., P. Molnar, 1977. Active faulting and tectonics in China. J. Geophys. Res. 82, n°20,
193 2905-2930.
194 Van der Woerd, J., P. Tapponnier, F.J. Ryerson, A.-S. Mériaux, B. Meyer, Y. Gaudemer,
195 R.C. Finkel, M.W. Caffee, Zhao G., Xu Z., 2002. Uniform Post-Glacial slip-rate along
196 the central 600 km of the Kunlun Fault (Tibet), from ^{26}Al,^{10}Be and ^{14}C dating of riser
197 offsets, and climatic origin of the regional morphology. Geophys. J. Int. 148, 356-388.
198 Wager, L.R., 1937. The Arun River Drainage Pattern and the Rise of the Himalaya. The
199 Geographical Journal 89 (3), 239-250.
200 Yin, A., T.M. Harrison, F.J. Ryerson, Chen W., W.S.F. Kidd, P. Copeland, 1994. Tertiary
201 structural evolution of the Gangdese thrust system, southeastern Tibet. J. Geophys. Res.
202 99, 18175-18201.

Figure captions

Figure 1 : Simplified geological and active fault map of the Dinggye region (see inset for location within Indo-Asia collision framework). The Gongzuo and Comuzhelin basins are characterized by folds, trending on average EW, of the Tethysian sediments in the hanging wall of the north dipping south Tibetan detachment system (e.g., Burg et al., 1984). Present-day active faults are NS trending normal faults (e.g. Armijo et al., 1986). Note the extension of high lake stands (at 4400 and 4460 m a.s.l.) marked by clear shorelines (sand bars, steep cliffs, etc…). Arrow is location of figure 2. Rectangles are figures 3, 4 and 5.

Figure 2 : Large river bed cannot be used to infer tectonic left-lateral displacement. River is deflected due to the bedrock outcrop partialy damming the valley at the foot of the bajada (note ~E-W bedding in bedrock). Unconstrained bounds of the deflection range from 0 to 5.7 km.

Figure 3 : Example of colluvial slope-deposits indurated by a calcareous matrix along the 4400 m a.s.l. paleo-lake shore line (see figure 1 for location). These are typical around the paleo-lake and have been mis-interpreted by Li and Yin (2008) as a scarp along an active fault trace. Arrow is location of inset.

Figure 4 : A) Interpretation of the Northern Gongzuo basin region. B) High resolution image of the site of terrace offsets described by Li and Yin (2008). C) High resolution image interpretation showing the unreliable interpretation of Li and Yin (2008). No active fault is

crossing the area, stream has barely formed any terrace. White arrows indicate inferred trace of active fault by Li and Yin (2008).

Figure 5 : Detail of the western part of Comuzhelin lake (see figure 1 for location). A) Landsat satellite image enhancement. B) Interpretation of image. Note uppermost shoreline (here a proeminent sand bar) wrongly mapped by Li and Yin (2008) in their Fig. 5 : the apparent horizontal separation is not left-lateral but right-lateral across the roughly EW elongated sedimentary bedrock out-crop itself interpreted as a strike-slip fault. Square is figure 5C. C) High resolution image enhancement from GoogleEarth of upper paleo-lake shoreline on western shore of Comuzhelin lake (see location in figure 3). Arrows point to clear sand bars that show a right step across EW trending bedrock outcrop that cannot be interpreted as a left-lateral offset as suggested by Li and Yin (2008). No evidence of EW fault trace can be seen despite the high resolution of the image (pixel size of about 1 m).

Figure 6 : A) plot of GPS velocities in southern Tibet (velocities from Zhang et al., [2004] projected relative to station JANK). Green vectors for stations west of Ama Drime massif. Background is Figure 2 of Li and Yin (2008). B) projection of EW componentof velocities on a N-S profile (eastward values are positive). Velocities show no left-lateral component across the DCFZ. There may exist a strike-slip component, it is right lateral and significant only for stations located north of the suture zone (YSZ). The relative velocity between stations (JIAN, LAZE, XIGA) and stations (JANK,DELO,YADO, KHAN) amounts about 2 mm/yr right-laterally (ignoring error bars).

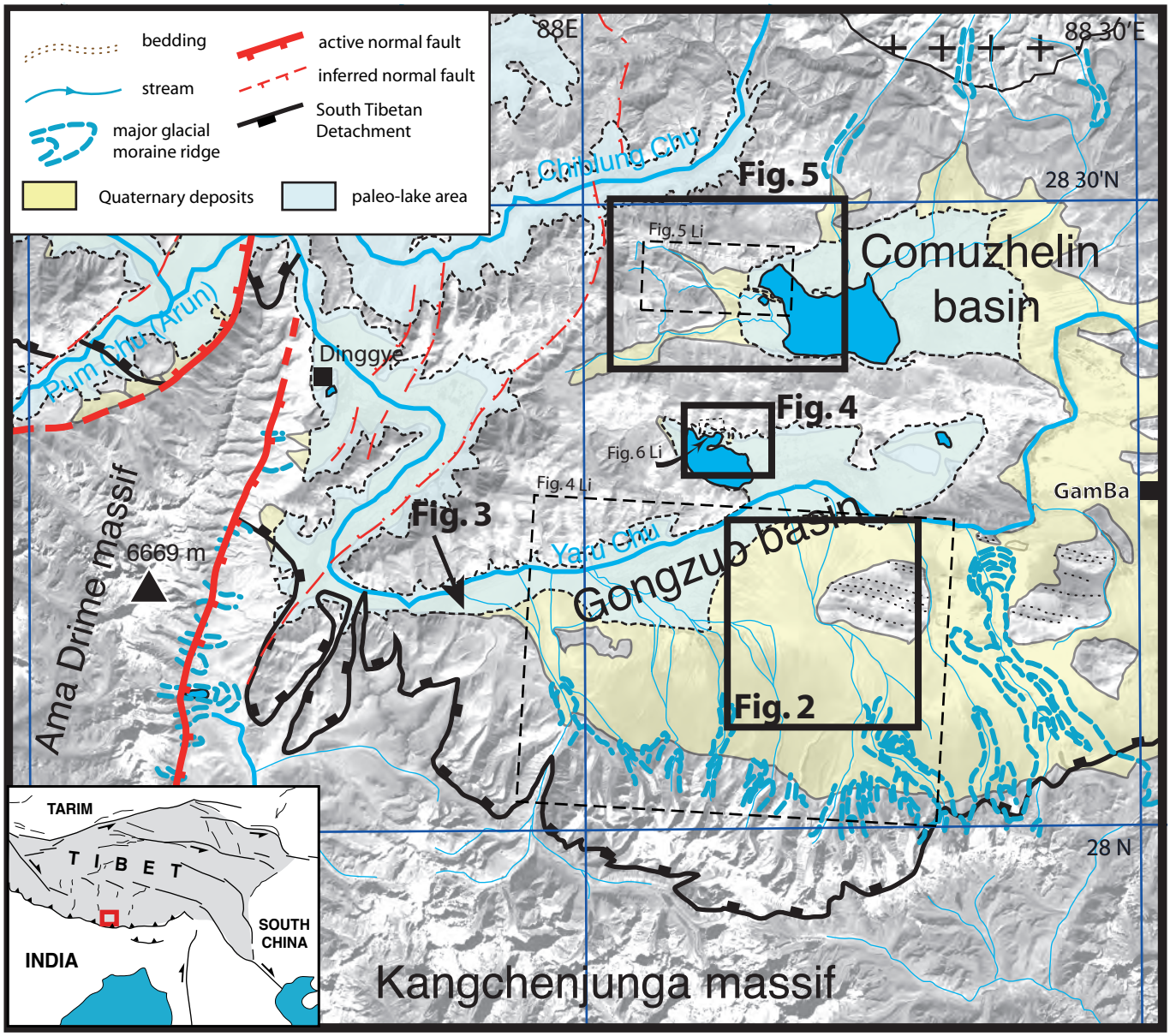
bedding
stream
major glacial moraine ridge
active normal fault
inferred normal fault
South Tibetan Detachment
Quaternary deposits
paleo-lake area
88E
88 30'E
28 30'N
28 N
Chhulung Chu
Fig. 5
Fig. 5 Li
Comuzhelin basin
Rum Chu (Arun)
Dinggye
Fig. 4
Fig. 6 Li
Fig. 4 Li
GamBa
Fig. 3
Ama Drime massif
6669 m
Yaru Chu
Gongzuo basin
Fig. 2
TARIM
T I B E T
SOUTH CHINA
INDIA
Kangchenjunga massif

Figure 1

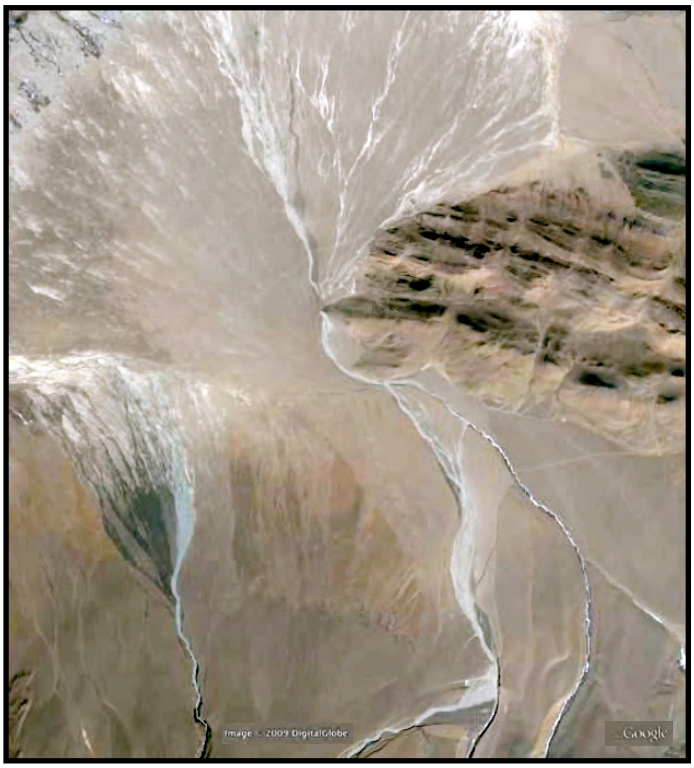
Image © 2009 DigitalGlobe
Google

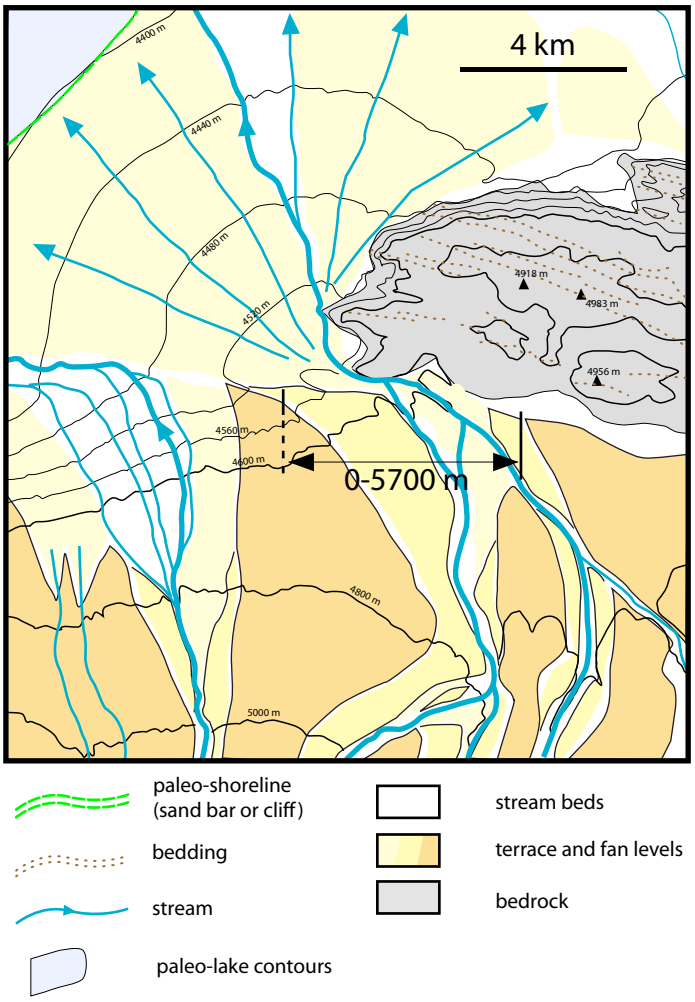
4 km
4400 m
4440 m
4460 m
4520 m
4560 m
4600 m
4800 m
5000 m
4918 m
4983 m
4956 m
0-5700 m
paleo-shoreline
(sand bar or cliff)
bedding
stream
paleo-lake contours
stream beds
terrace and fan levels
bedrock

Figure 2

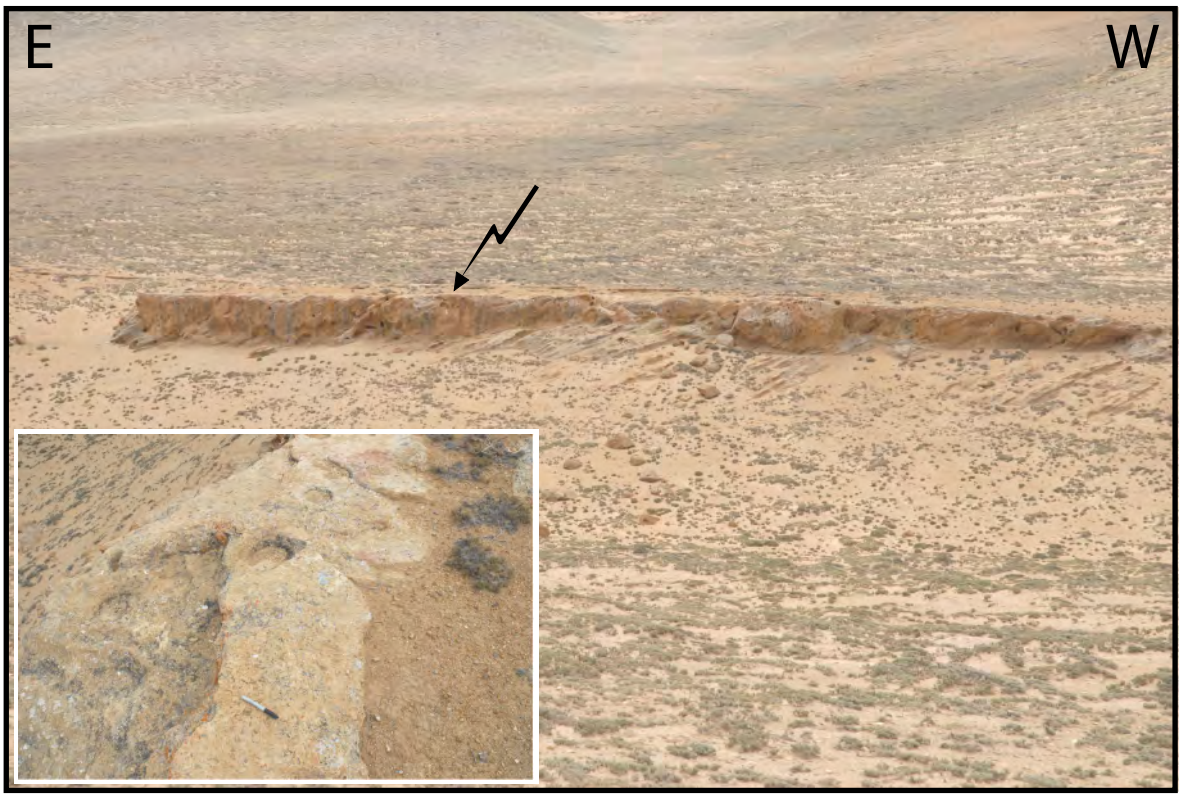

Figure 3

A

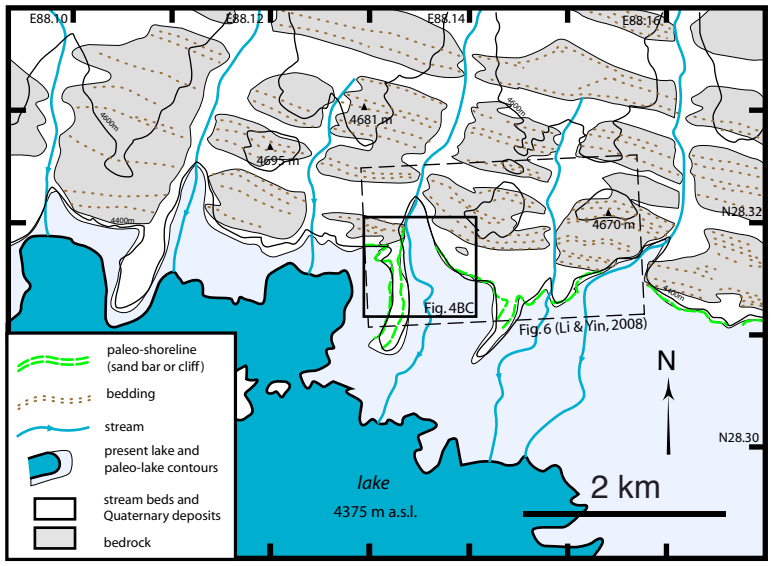

B

C

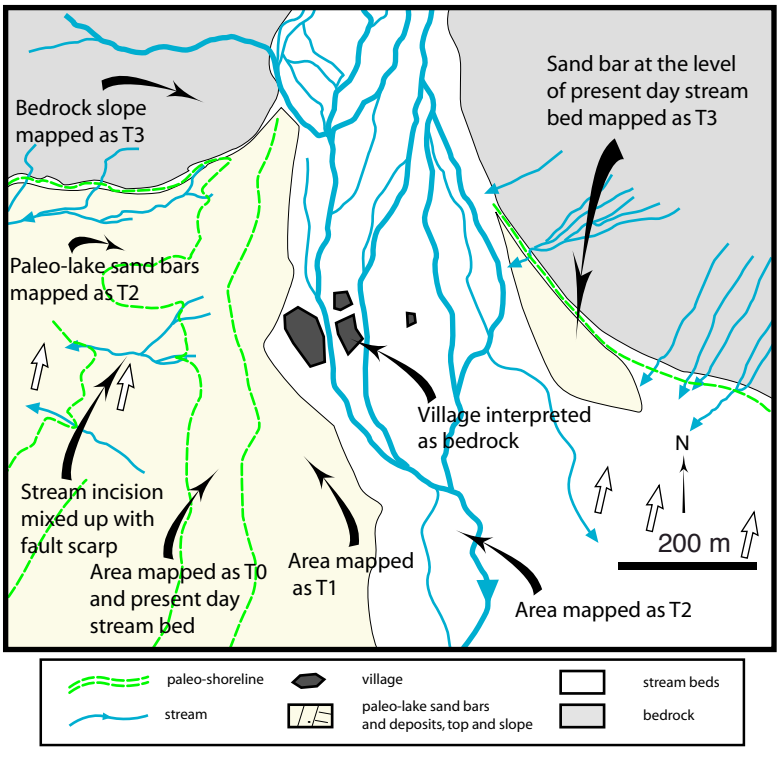

Figure 4ABC

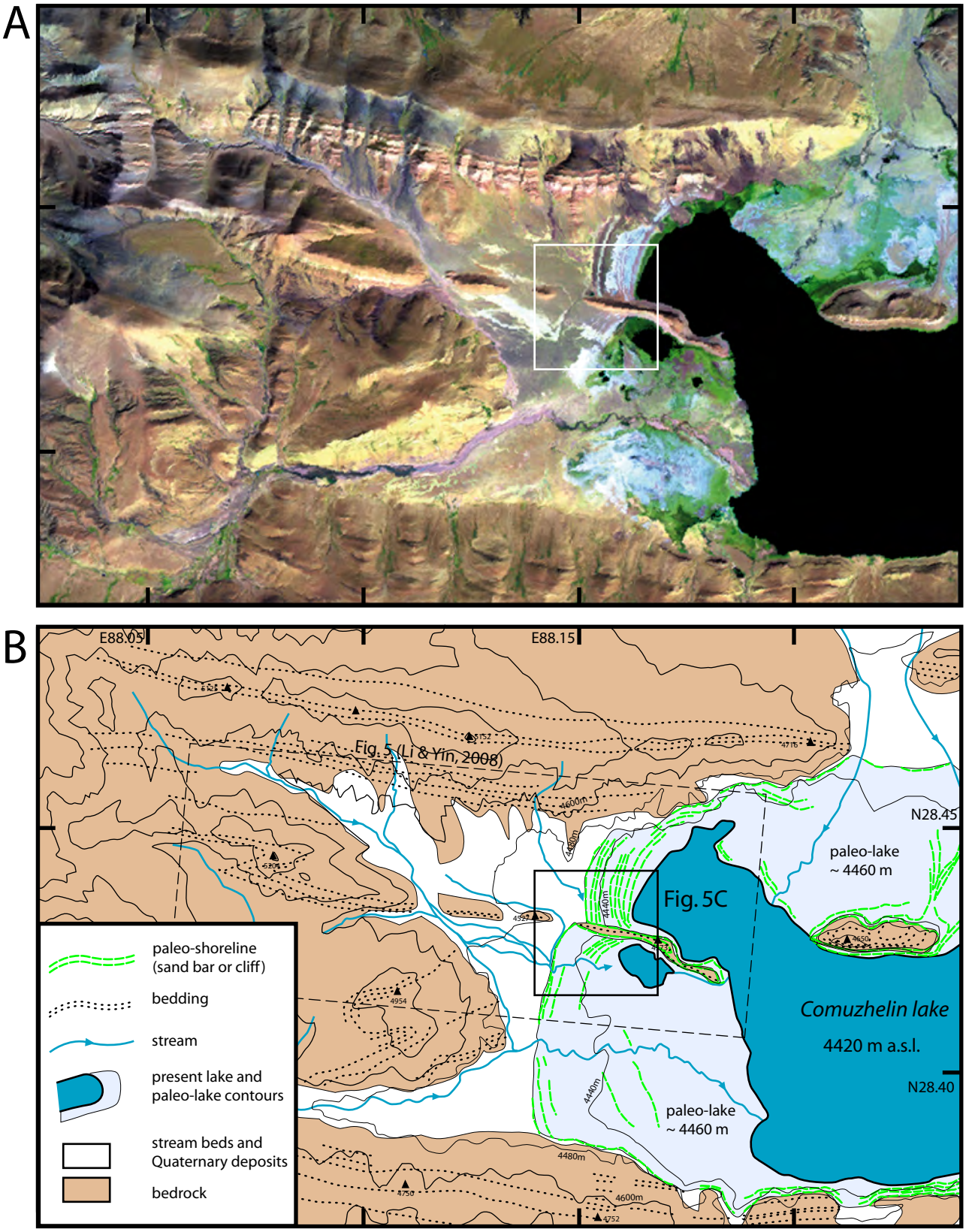
A
B
E88.05
E88.15
N28.45
N28.40
Fig. 5 (Li & Yin, 2008)
Fig. 5C
paleo-lake
~ 4460 m
Comuzhelin lake
4420 m a.s.l.
paleo-lake
~ 4460 m
4600m
4480m
4440m
4460m
paleo-shoreline
(sand bar or cliff)
bedding
stream
present lake and
paleo-lake contours
stream beds and
Quaternary deposits
bedrock

Figure 5AB

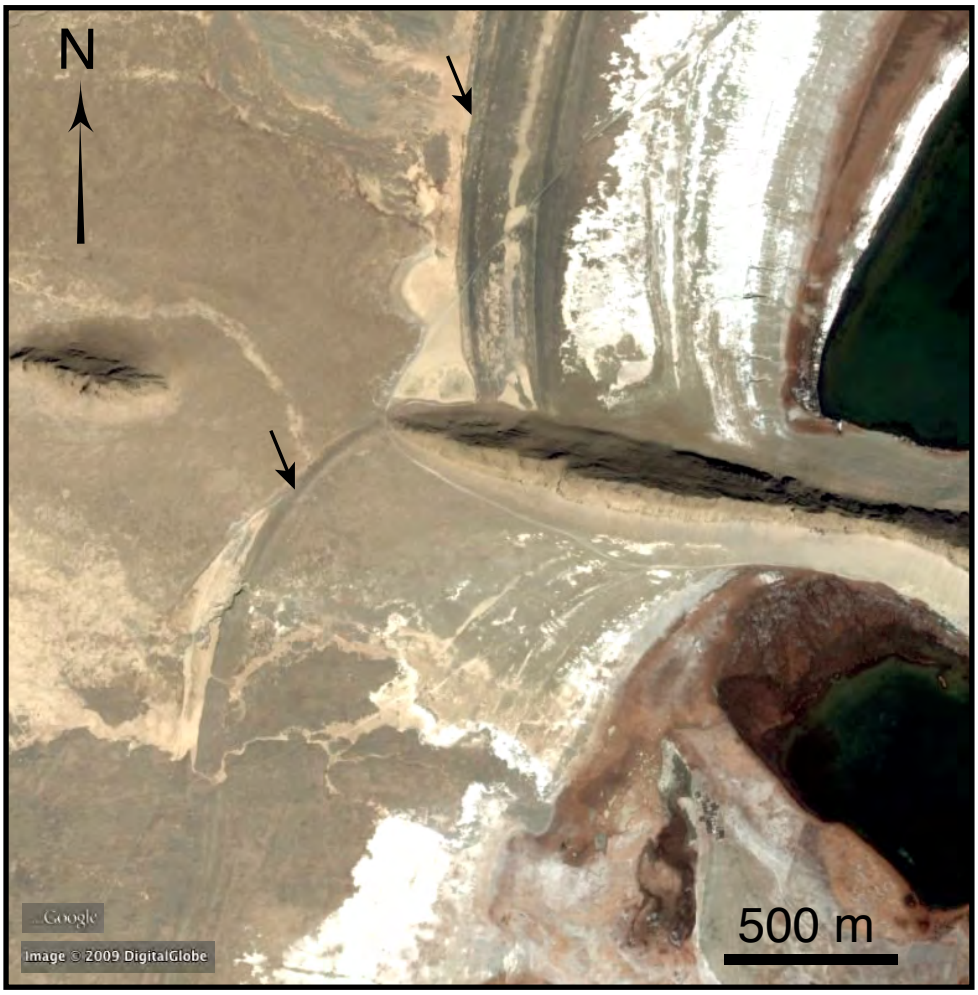

Figure 5C

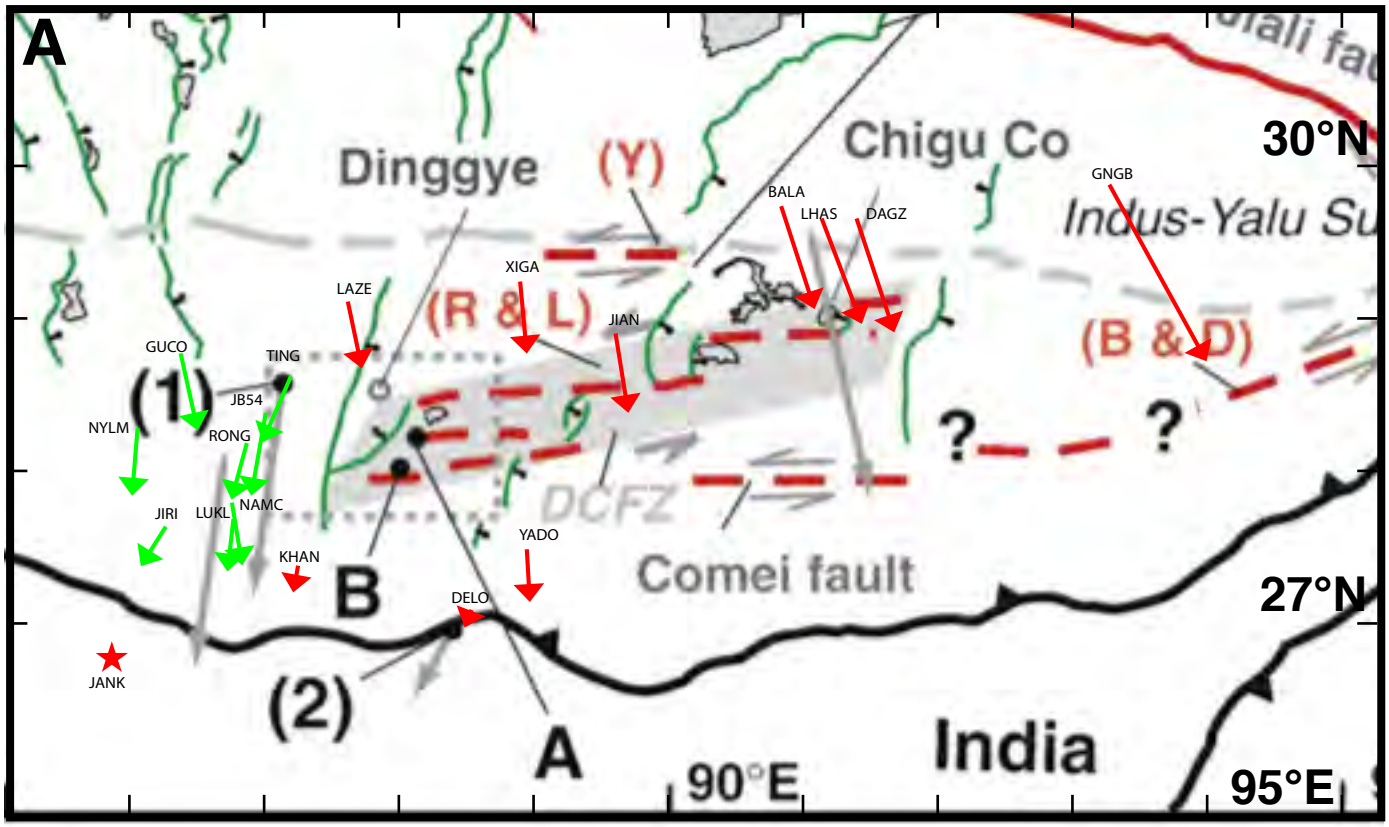
A
Dinggye
(Y)
Chigu Co
30°N
GNGB
BALA
LHAS
DAGZ
Indus-Yalu Su
XIGA
LAZE
(R & L)
JIAN
(B & D)
GUCO
TING
(1)
JB54
NYLM
RONG
?
?
JIRI
LUKL
NAMC
DCFZ
YADO
KHAN
B
Comei fault
27°N
DELO
JANK
(2)
A
India
90°E
95°E

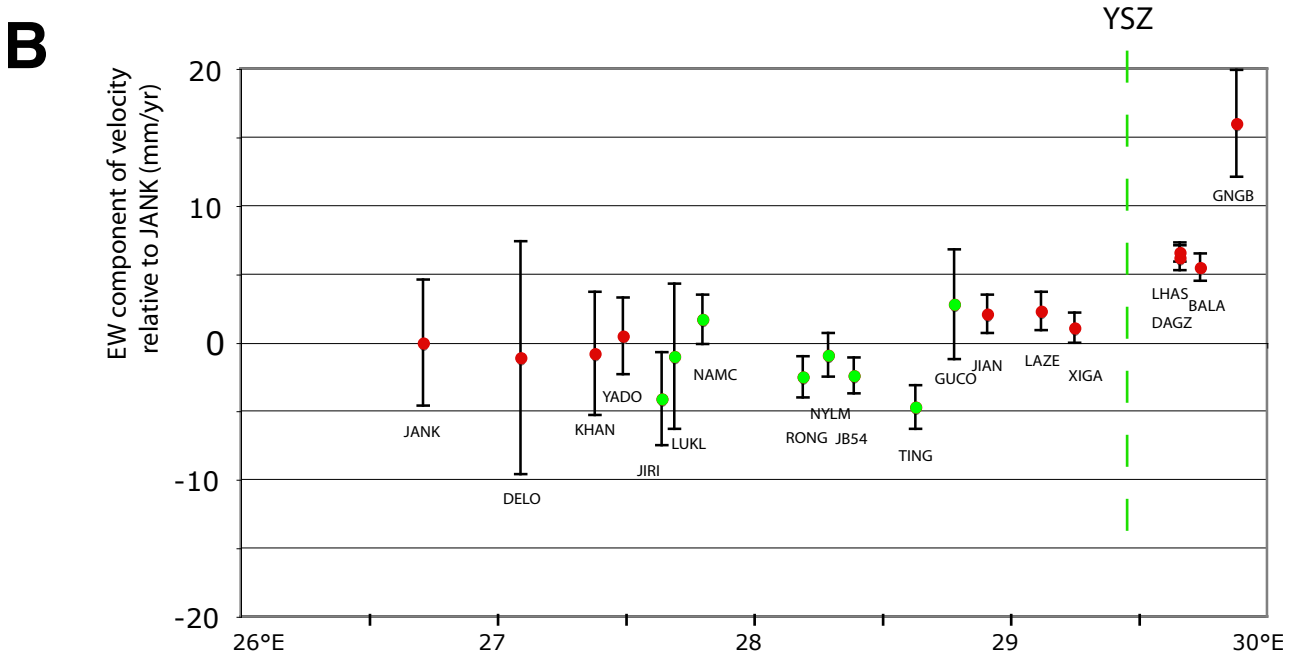
B
YSZ
EW component of velocity
relative to JANK (mm/yr)
20
10
0
-10
-20
26°E
27
28
29
30°E
GNGB
LHAS
BALA
DAGZ
JANK
DELO
KHAN
YADO
JIRI
LUKL
NAMC
NYLM
RONG
JB54
TING
GUCO
JIAN
LAZE
XIGA

Figure 6